Parkinson's Disease Development Prediction by C-Granule Computing

Andrzej W. Przybyszewski[1,2(✉)]

[1] Polish-Japanese Academy of Information Technology, 02-008 Warsaw, Poland
przy@pjwstk.edu.pl
[2] Department of Neurology UMass Medical School, Worcester, MA 01655, USA

Abstract. Both Rough Set Theory (RST) and Fuzzy Rough Set Theory (FRST) are related to intelligent granular computing (GrC) but primary with help of static granules. Our granules are sets of attributes measured from Parkinson's disease (PD) patient in a certain moment of his/her disease. In order to look into PD development in time during our longitudinal study, we have introduced the complex granule (c-granule) approach with properties of granules that are evolving with disease progression.

We have used a RST/FRST approach in order to find similarities between attributes of different patients in different disease stages to another group of more advanced PD patients. We have compared group (G1) of 23 PD with attributes measured three times (visits V1 to V3) every half of the year (G1V1, G1V2, G1V3) to other group of 24 more advanced PD (G2V1). By means of RST/FRST we have found rules describing symptoms of G2V1 and applied them to G1V1, G1V2, and G1V3. With RST (FRST) we've got the following accuracies: G1V1 – 59 (38)%; G1V2 – 68(54)%; G1V3 – 86(61)% but global coverage for FRST was better. This means that c-granule attributes became more similar to the model.

Keywords: Granular computing · Similarity · Aggregation · Disease progression · Disease model

1 Introduction

Our goal was to simulate Parkinson's disease (PD) development in time with help of granular computing (GrC) methods [1, 2]. As PD related neurodegeneration (ND) starts about 20 years before first symptoms and during this period of time ND process is effectively compensated by brain plasticity, each patient's PD progressions are different.

In this work, we have used intelligent granular computing based on the principle of complex object classifications from the visual brain [3, 4]. As states in the schematic (Fig. 1) properties of the unknown object p are represented as α and compared with the model α_M (in the brain – possible objects [3], here symptoms of more advanced PDs). It results rules β that determine new object's properties or PD time development.

N. T. Nguyen et al. (Eds.): ICCCI 2019, LNAI 11683, pp. 1–11, 2019.
https://doi.org/10.1007/978-3-030-28377-3_24

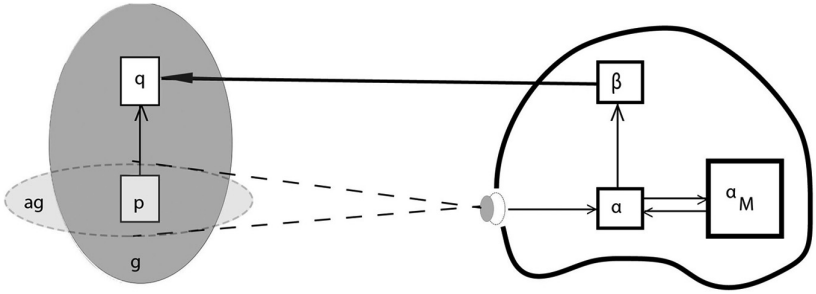

Fig. 1. It is a principal schematic of the intelligent granular computing base on the brain intelligence. We observe a limited part of c-granule g that is generally subpart ag of environment env in a time interval [t − **Δ**, t]. Interaction between env and ag in time t during **Δ** Int g,t,Δ (env, ag) represents α and results that rule *(α ∩ α_M, γ)−>β* is learned by ag, where γ represents properties of the structure g, and α property of the interaction process, and β describes unknown, expected properties other part of g that might be reason for future changes into the disease; α_M it is the model of the world that interacts with α in order to extracts its significant features (modified after [5]).

2 Methods

Our data mining analysis is based on granular computing implemented in RST (rough set theory proposed by Pawlak [1] and FRTS (fuzzy rough set theory) by extending RST indiscernibility with concepts of the tolerance Zadeh [2].

Our data is converted to the decision table where rows were related to different measurements and columns represent different attributes. An information system [1] a pair $S = (U, A)$, where *U, A* are nonempty finite sets called the universe of objects *U* and the set of attributes *A*. If $a \in A$ and $u \in U$, the value a(u) is a unique element of *V* (where V is a value set).

We define as in [1] for RST the indiscernibility relation of any subset *B* of *A* or *IND (B) as:* $(x, y) \in$ *IND(B) or xI(B)y iff a(x) = a(y)* for every $a \in B$ where the value of $a(x) \in V$. It is an equivalence crisp relation $[u]_B$ that we understand as a B-elementary granule. The family of $[u]_B$ gives the partition *U/B* containing u will be denoted by *B (u).* The set $B \subset A$ of information system S is a reduct *IND(B) = IND(A)* and no proper subset of B has this property [1]. In most cases, we are only interested in such reducts that are leading to expected rules (classifications). On the basis of the reduct we have generated rules using four different ML methods (RSES 2.2): exhaustive algorithm, genetic algorithm, covering algorithm, or LEM2 algorithm.

A *lower approximation* of set $X \subseteq U$ in relation to an attribute B is defined as all elements have B attribute: $\underline{B}X = \{u \in U : [u]_B \subseteq X\}$. The upper approximation of X is defined as some elements have B attribute: $\overline{B}X = \{u \in U : [u]_B \cap X \neq \phi\}$. The difference of $\overline{B}X$ and $\underline{B}X$ is the boundary region of X that we denote as $\mathrm{BN_B(X)}$. If $BN_B(X)$ is empty then set than X is exact with respect to B; otherwise if $\mathrm{BN_B(X)}$ is not empty and X is not rough with respect to B.

A decision table (training sample in ML) for S is the triplet: $S = (U, C, D)$ where: *C, D* are condition and decision attributes [1]. Each row of the decision table gives a particular rule that connects condition and decision attributes for a single measurements, RST generalizes these particular rules into universal hypotheses (object or disease classification.

Dubois and Prade [6] have generalized RST to FRTS (fuzzy rough set theory) by extending RST indiscernibility with concepts of tolerance after Zadeh's membership degrees in fuzzy sets [2].

As the consequence, 'crisp' dependences were replaced by a fuzzy tolerance or similarity relations Ra(x, y) as a value between two observations x and y. As Ra(x, y) is a similarity relation, it must be reflexive, symmetric and transitive. As summarized in [7] there are several tolerance relationships such as the normalized difference (so-called 'Eq. 1') or Gaussian or exponential differences [7]. There are also formulas related to normalized differences between pairs of attributes. The most common are **Łukasiewicz (t.norm)** and **t.cos** $-\tau$ [7]. As decision attributes are nominative we used crisp relations between them.

We define B-lower and B-upper approximations for each observation x in FRST as following: *B-lower* approximation as:$(R_B)(x) = \inf_{y \in U} I(R_B(x, y), X(y))$ where I is an *implicator* [7]. The B-lower approximation for the observation x is then the set of observations, which are the most similar to observation x and it can predict the decision attribute with the highest confidence, based on conditional attributes B.

The B-upper approximation is defined by $(R_B)(x) = \sup_{y \in U} \tau(R_B(x, y), X(y))$, where τ is the t-norm. The B-upper approximation is a set of observations for which the prediction of decision attribute has the smallest confidence [7].

Notice that rules in FRST have dissimilar formation than in RST. They are based on the tolerance classes and appropriate decision concepts. The fuzzy rule is a triple (B, C, D), where B is a set of conditional attributes that appear in the rule, C stands for fuzzy tolerance class of object and D stands for decision class of object.

We have used RST algorithms implemented as the RSES 2.2 (logic.mimuw.edu.pl/~rses/get.html) Exploration Program Rough System and FRST implemented as Rough Set package in R [7].

2.1 Measured Attributes

We have tested two groups of PD patients: the first group (G1) of 23 patients was measured three times every half of the year (visits were numbered as V1, V2, V3), and the second group (G2) had more advanced 24 patients and were a reference model of disease progression in the first group. Both groups of patients were only on medication. The major medication in this group was L-Dopa that increases concentration of the transmitter dopamine in the brain as it that is lacking in Parkinson's patients. In the most cases PD starts with neurodegeneration in substantia nigra that is responsible for the release of the dopamine.

All patients were measured in two sessions: MedOFF (session S#=1 without -medication) and MedON (session S#=2 patients on medications). In addition all

patients have the following procedures: neuropsychological tests: PDQ39 (quality of life), Epworth (sleepiness test); neurological tests: eye movements and standard PD test: UPDRS (Unified Parkinson's Disease Rating Scale). All tests were performed in Brodno Hospital, department of Neurology, Faculty of Health Science, Medical University Warsaw, Poland. In the present work, we have tested and measured fast eye movements: reflexive saccades (RS) as described in our previous publications [8, 9]. In summary, every subject was sitting in a stable position without head movements and watching a computer screen before him/her. At the beginning he/she has to fixate in the center of the screen, and to keep on moving light spot. This spot was jumping randomly, ten degrees to the right or ten degrees to the left. Patient has to follow movements of the light spot and following parameters were measured: latency (RSLat) – time difference between beginning of spot and eyes movements, saccade duration (RSDur); saccade amplitude (RSAmp) and saccade velocity (RSVel).

3 Results

For the first group of PD patients we have performed three tests, every half-year, whereas the second group of more advanced PD we have measured only one time. The mean age of the first group (G1) was 57.8+/−13 (SD) years with disease duration 7.1+/−3.5 years; UPDRS MedOff/On was 48.3+/−17.9 and 23.6+/−10.3 for the first visit (V1); 57.3+/−16.8 and 27.8+/−10.8 for the second visit (V2), 62.2+/−18.2 and 25+/−11.6 for the third visit (V3). The second group (G2) of patients was more advanced with mean age 53.7+/−9.3 years, and disease duration 10.25+/−3.9 years; UPDRS MedOff/On was 62.1+/−16.1 and 29.9+/−13.3 measured one time only. Data were placed in four information tables: G1V1, G1V2, G1V3, and G2V1.

Table 1. Part of the decision table for three G1V1 patients

P#	Ses	tdur	PDQ39	Epworth	RSLat	RSDur	RSAmp	RSVel	UPDRS
10	1	5.3	90	17	205	51	9.8	343	58
10	2	5.3	90	17	182	56	10	333	35
11	1	15	122	8	245	55	12	503	57
11	2	15	122	8	266	55	12	431	40
12	1	5.5	20	3	178	54	10	421	25
12	2	5.5	20	3	161	58	13	505	15
13	1	4.8	68	9	299	59	13	472	46
13	2	4.8	68	9	234	57	11	367	26

Table 1 has 46 rows: 23 patients measured in two sessions each. Condition attributes patient number P#, S# session number, tdur – disease duration, PDQ39, Epworth (as above), RS parameters (above). The decision attribute is UPDRS that is proportional to the disease progression, it increases from G1V1 to G1V3 and it will be referred to G2V1.

3.1 Rough Set Approach

In the next step, Table 1 is discretized by RST and part of the table for G1V1 patients in Table 2 below. Notice that some less significant attributes were by algorithm of RSES 2.2 discarded: RSDur, RSAmp, and RSVel – duration, amplitude and velocity of reflexive saccades.

Table 2. Discretized-table Table 1 for three G1V1 patients

P#	Ses	tdur	PDQ39	Epworth	RSLat	RSDur	RSAmp	RSVel	UPDRS
10	1		"(-Inf,5.65)"	"(50.5,Inf)"	"(14,Inf)"	"(-Inf,264)"	* * *		"(43,63)"
10	2		"(-Inf,5.65)"	"(50.5,Inf)"	"(14,Inf)"	"(-Inf,264)"	* * *		"(33.5,43)"
11	1		"(5.65,Inf)"	"(50.5,Inf)"	"(-Inf,14)"	"(-Inf,264)"	* * *		"(43,63)"
11	2		"(5.65,Inf)"	"(50.5,Inf)"	"(-Inf,14.)"	"(264,Inf)"	* * *		"(33.5,43)"
12	1		"(-Inf,5.65)"	"(-Inf,50.5)"	"(-Inf,14)"	"(-Inf,264)"	* * *		"(-Inf,33.5)"
12	2		"(-Inf,5.65)"	"(-Inf,50.5)"	"(-Inf,14)"	"(-Inf,264)"	* * *		"(-Inf,33.5)"
13	1		"(-Inf,5.65)"	"(50.5,Inf)"	"(-Inf,14.0)"	"(264,Inf)"	* * *		"(43,63)"
13	2		"(-Inf,5.65)"	"(50.5,Inf)"	"(-Inf,14.)"	"(-Inf,264)"	* * *		"(-Inf,33.5)"

By means of the discretization RSES software RSES 2.2 (see Methods) UPDRS was divided into 4 ranges: "(-Inf, 33.5)", "(33.5, 43.0)", "(43.0, 63.0)", and "(63.0, Inf)". All other attributes, except symbolic attributes P# (number given to each patient) and S# (session number) were also discretized (Table 2).

Cross validation (6-fold) based on the decomposition tree of the first visit G1V1 data gave the global accuracy 0.896 and global coverage 0.35. Prediction, based on rules from G1V1, of UPDRS in G1V2 and G1V3 gave global accuracy 0.7 with coverage 1, and these results do not indicate time related disease progression.

For G2V1 group rules from G1V1 gave global accuracy 0.64 and coverage 0.5. However, it was more interesting to estimate G1V1 to G1V3 from other more advanced model group of patients G2V1.

This way we can follows our c-granular approach (Fig. 1) where the model are granules of attributes of G2V1 that might predict PD time: G1V1, G1V3, G1V3 development. With help of RSES we have found rules describing relationships between condition and decision attributes in G2V1 and we are using these rules to predict disease symptoms in G1 group for each visit V1, V2, and V3. If the disease progression has direction going to the model (G2V1) group then are predictions should increase with the time of the disease. We demonstrate our predictions in three following Tables 3, 4 and 5.

Table 3. Confusion matrix for UPDRS of G1V1 patients by rules obtained from G2V1 patients with RST

Actual	Predicted				
	"(63.0, Inf)"	"(33.5, 43.0)"	"(43.0, 63.0)"	"(-Inf, 33.5)"	ACC
"(63.0, Inf)"	2.0	0.0	0.0	0.0	1.0
"(33.5, 43.0)"	1.0	0.0	1.0	1.0	0.0
"(43.0, 63.0)"	6.0	0.0	1.0	0.0	0.14
"(-Inf, 33.5)"	3.0	0.0	2.0	17.0	0.77
TPR	0.17	0.0	0.25	0.94	

TPR: True positive rates for decision classes; ACC: Accuracy for decision classes: the global accuracy was 0.59 and global coverage was 0.74

Table 4. Confusion matrix for UPDRS of G1V2 patients by rules obtained from G2V1 patients with RST

Actual	Predicted				
	"(63.0, Inf)"	"(33.5, 43.0)"	"(43.0, 63.0)"	"(-Inf, 33.5)"	ACC
"(63.0, Inf)"	3.0	0.0	1.0	0.0	0.75
"(33.5, 43.0)"	0.0	0.0	2.0	1.0	0.0
"(43.0, 63.0)"	4.0	0.0	0.0	0.0	0.0
"(-Inf, 33.5)"	0.0	0.0	1.0	16.0	0.94
TPR	0.43	0.0	0.0	0.94	

TPR: True positive rates for decision classes; ACC: Accuracy for decision classes: the global accuracy was 0.68 and global coverage was 0.61.

Table 5. Confusion matrix for UPDRS of G1V3 patients by rules obtained from G2V1 patients with RST

Actual	"(63.0, Inf)"	"(33.5, 43.0)"	"(43.0, 63.0)"	"(-Inf, 33.5)"	ACC
"(63.0, Inf)"	3.0	0.0	0.0	0.0	1.0
"(33.5, 43.0)"	0.0	0.0	1.0	2.0	0.0
"(43.0, 63.0)"	0.0	0.0	0.0	0.0	0.0
"(-Inf, 33.5)"	0.0	0.0	2.0	16.0	1.0
TPR	1.0	0.0	0.0	1.0	

TPR: True positive rates for decision classes; ACC: Accuracy for decision classes: the global accuracy was 0.86 and global coverage was 0.48.

In Table 3 are prediction of the UPDRS for the first visit group of patients (G1V1). Notice that in this and two other tables (Tables 4 and 5) we could not predict UPDRS between 33.5 and 43. The accuracy in Table 3 was below 60%, but it increases for each following visit: G1V2 has global accuracy 68% and G1V3 – 86%. Therefore patients' symptoms become with time more similar to G2V1 group.

An important part in these estimations is to find rules that are enough general to be patient independent (there are different patients in G1 and G2 groups) and not too general in order to find differences between different visits.

There were all together 71 rules, e.g.

$$(Ses=2)\&(PDQ39="(-Inf,50.5)")=>(UPDRS="(-Inf,33.5)"\ [10]) \tag{1}$$

$$(Ses=2)\&(Epworth="(-Inf,14.0)")\&(RSLat="(264.0,Inf)") \\ =>(UPDRS="(63.0,Inf)"[4]) \tag{2}$$

$$(dur="(5.65,Inf)")\&(Ses=2)\&(RSLat="(-Inf,264.0)") \\ =>(UPDRS="(-Inf,33.5)"[14]) \tag{3}$$

$$(Ses=1)\&(PDQ39="(-Inf,\ 50.5)")\&(RSLat="(264.0,Inf)") \\ =>(UPDRS="(63.0,Inf)"[1]) \tag{4}$$

Equations (1–3) were for *Ses = 2* (patient on medication) and they were fullfield by 10 (1), 4 (2) and 14 (3) cases, whereas Eq. 4 was for 1 case only.

We can read (1) as for patients on medication *(Ses = 2)* and with *PDQ39* (quality of life test result) smaller than *50.5* then his/her *UPDRS will be smaller than 33.5.*

3.2 Fuzzy Rough Set Approach

We have obtained our predictions using the generalized fuzzy rough set rules (GFRS) with aggregation by the t.norm **Łukasiewicz**, similarity expressed as tolerance Eq. 3 (modified Gaussian from [7]), and implicator – Łukasiewicz; alpha precision was 0.05. As the decision attribute must be nominal, so we have chosen classes that are similar to already used in our previous section: "(-Inf, 33.5)' = "1"; "(33.5, 43.0" = "2"; "(43.0, 63.0)" = "3",: "(63, Inf)" = "4". The examples of FRST rules are below:

$$(Ses=1)\&(Epworth =''16")\&(RSLat="192") =>(UPDRS="3") \tag{5}$$

$$(Ses=2)=>(UPDRS="1") \tag{6}$$

$$(Ses=1)\&\ (Epworth =''1")\&(RSLat="289") =>(UPDRS="4"\ ) \tag{7}$$

We can read Eq. (5) as for patients without medication (s#=1) and with Epworth (quality of sleep test result) about 16 and saccade latency about 192 then his/her UPDRS will be about 3 (between 34 and 63).

FRST rules have some similarities to RST rules but there are not 'crisp' there are fuzzy and more difficult to interpret as their fuzziness are not given directly as they are dependent on aggregation, tolerance and implicator equations. Their advantage to RST rules is that they cover all cases with the global coverage = 1. As above we have found FRST rules for our model group of patients G2V1 and applied these rules to other groups G1V1, G1V2, and G1V3 (Tables 6, 7 and 8).

Accuracies of out FRST predictions were inferior in comparison to FRS predictions, but as before accuracy is increasing with each visit: G1V1 – accuracy was below 40%, for G1V2 – 54% and for G1V3 visit was over 60%. Also notice that we did not get right predictions for UPDRS nominal values 2 and 3 that were between (33.5 and 43) and between (43 and 63), but we have got relatively good predictions for classes 1 and 4 were accuracy for decision classes ACC was almost for all estimations near 1.

Table 6. Confusion matrix for UPDRS of G1V1 patients by rules obtained from G2V1 patients with FRST

Actual	Predicted				
	"1"	"2"	"3"	"4"	ACC
"1"	19	0	0	5	0.79
"2"	2	0	0	4	0.0
"3"	2	0	0	11	0.0
"4"	0	0	0	3	1
TPR	0.826	0.0	0.0	0.13	

TPR: True positive rates for decision classes; ACC: Accuracy for decision classes: the global accuracy was 0.38 and global coverage was 1.

Table 7. Confusion matrix for UPDRS of G1V1 patients by rules obtained from G2V1 patients with FRST

Actual	Predicted				
	"1"	"2"	"3"	"4"	ACC
"1"	18	0	0	0	1.0
"2"	4	0	0	2	0.0
"3"	2	0	0	13	0.0
"4"	0	0	0	7	1.0
TPR	0.75	0.0	0.0	0.32	

TPR: True positive rates for decision classes; ACC: Accuracy for decision classes: the global accuracy was 0.54 and global coverage was 1.

Table 8. Confusion matrix for UPDRS of G1V3 patients by rules obtained from G2V1 patients with FRST

Actual	Predicted				
	"1"	"2"	"3"	"4"	ACC
"1"	17	0	0	0	1.0
"2"	5	0	0	3	0.0
"3"	2	0	0	8	0.0
"4"	0	0	0	11	1.0
TPR	0.74	0.0	0.0	0.5	

TPR: True positive rates for decision classes; ACC: Accuracy for decision classes: the global accuracy was 0.61 and global coverage was 1.

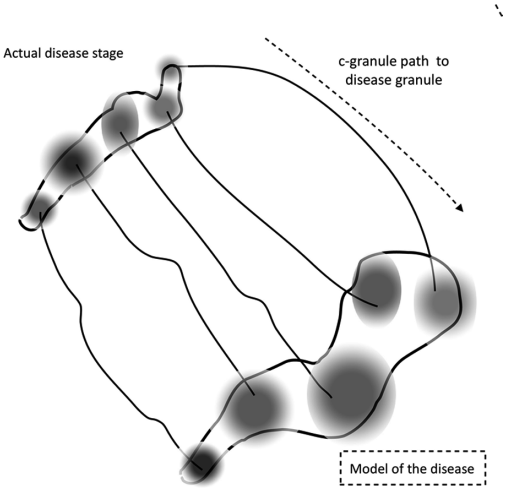

Fig. 2. C-granule path in disease development compared to the model

4 Discussion

In this work we have used c-granular computing to estimate disease progression in time (longitudinal study) of patients with Parkinson's disease (PD). As in each individual PD symptoms and their developments are different **("No two people face Parkinson's in quite the same way")** we would like to know if we could predict a particular patient progression by looking to more advanced group of patients.

We have used granular computing (GrC) with RST (rough set theory) and FRST (fuzzy rough set theory). RST looks into 'crisp' granules and estimates objects by upper and lower approximations that determine precision of the description as dependent from properties of granules. Therefore RST can give very precise estimation

but not for all objects (patients). This we can see in our results where we can precisely predict symptoms (measured as UPDRS) of patients, but not all of them (global coverage less than 1). If we make our granules fuzzy (not crisp) they can describe properties of all objects (patients) with global coverage = 1, but less precisely. Our present results might be a good example of these differences.

Another important aspects of our approach are similarities between findings all-important aspects (symptoms) of the disease and recognition of the complex object (Fig. 1). In the visual brain we are trying to infer not clear visible object's properties from attributes we have classified from a to b and back to a new part (q) of the object. However, it is a very important principle of our vision – the Model. It consists world, particular environment and known objects. We are able to precisely classify a complex, unknown object as we are tuning and comparing it particular attributes in many different levels (and even with different logics [1]). The model is important part of our approach. Our model is determined by attributes of the more advanced group of PD – G2V1. As it is illustrated in Fig. 2 granules describing different disease stages might develop or stay constant. In each disease stage we are comparing actual symptoms with the model and look for the similarities. We have demonstrated on group of over 20 patients that even if each one has different symptoms their path (c-granule) is going in the direction of our model.

Changing treatment it might push patient symptoms to the different path. In order to test such options we need several models and to measure how to change the treatment to direct patients to different model. By testing several different patient's groups, we have demonstrated that the certain long lasting treatments can change disease develop to new directions that are not similar to classical medication treatments [10].

In such cases one possible solution is to increase number of granules (dimension of attributes) but adding new attributes that might 'sense' new direction of the disease development. We are actually testing influence of the depression on the direction of the symptoms changes, as depression is characteristic not only for Parkinson's disease but also for more common Alzheimer's (AD) where late (after 65 years of age) onset AD (LOAD) is in 50% related to depression. Others have proposed similar AI predictive methods: to voice changes [11], by using supporting vector machine [12] or modular approach [13] based on interactions between motor and psychological tests [14, 15].

In summary, we have demonstrated that by using approach similar to the visual brain intelligence might give us a new way of look into similarities between different groups of patients. In addition, we might see longitudinal studies as c-granules and measure symptoms by distance to the Model (advance stage of the disease).

References

1. Pawlak, Z.: Rough Sets - Theoretical Aspects of Reasoning About Data. Kluwer Academic Publisher, Dordrecht (1991)
2. Zadeh, L.A.: From computing with numbers to computing with words - from manipulation of measurements to manipulation of perceptions. Int. J. Appl. Math. Comput. Sci. **12**, 307–324 (2002)

3. Przybyszewski, A.W.: The neurophysiological bases of cognitive computation using rough set theory. In: Peters, J.F., Skowron, A., Rybiński, H. (eds.) Transactions on Rough Sets IX. LNCS, vol. 5390, pp. 287–317. Springer, Heidelberg (2008). https://doi.org/10.1007/978-3-540-89876-4_16
4. Przybyszewski, A.W.: SI: SCA measures - fuzzy rough set features of cognitive computations in the visual system. J. Intell. Fuzzy Syst. (2018, pre-press). https://doi.org/10.3233/JIFS-18401
5. Skowron, A., Dutta, S.: Rough sets: past, present, and future. Nat. Comput. **17**, 855–876 (2018)
6. Dubois, D., Prade, H.: Rough fuzzy sets and fuzzy rough sets. Int. J. Gen. Syst. **17**, 91–209 (1990)
7. Riza, L.S., et al.: Implementing algorithms of rough set theory and fuzzy rough set theory in the R package RoughSets. Inf. Sci. **287**, 68–69 (2014)
8. Przybyszewski, A.W., et al.: Multimodal learning and intelligent prediction of symptom development in individual Parkinson's Patients. Sensors **16**(9), 1498 (2016). https://doi.org/10.3390/s16091498
9. Przybyszewski, A.W.: Fuzzy RST and RST rules can predict effects of different therapies in parkinson's disease patients. In: Ceci, M., Japkowicz, N., Liu, J., Papadopoulos, G.A., Raś, Z.W. (eds.) ISMIS 2018. LNCS (LNAI), vol. 11177, pp. 409–416. Springer, Cham (2018). https://doi.org/10.1007/978-3-030-01851-1_39
10. Przybyszewski, A.W., Szlufik, S., Habela, P., Koziorowski, D.M.: Multimodal learning determines rules of disease development in longitudinal course with parkinson's patients. In: Bembenik, R., Skonieczny, Ł., Protaziuk, G., Kryszkiewicz, M., Rybinski, H. (eds.) Intelligent Methods and Big Data in Industrial Applications. SBD, vol. 40, pp. 235–246. Springer, Cham (2019). https://doi.org/10.1007/978-3-319-77604-0_17
11. Tiwari, A.K.: Machine learning based approaches for prediction of Parkinson's disease. Mach. Learn. Appl. Int. J. (MLAIJ) **3**(2), 33–39 (2016)
12. Lerche, S., Heinzel, S., et al.: Aiming for study comparability in Parkinson's disease: proposal for a modular set of biomarker assessments to be used in longitudinal studies. Front. Aging Neurosci. (2016). https://doi.org/10.3389/fnagi.2016.00121
13. Singh, G., Vadera, M., Samavedham, L., Lim, E.C.: Machine learning based framework for multi-class diagnosis of neurodegenerative diseases: a study on Parkinson's disease. IFAC PaperOnLine **49**(7), 990–995 (2016)
14. Goldman, J.G., Holden, S., Ouyang, B., Bernard, B., Goetz, C.G., Stebbins, G.T.: Diagnosing PD-MCI by MDST ask force criteria: how many and which neuropsychological tests? Mov. Disord. **30**, 402–406 (2015)
15. Lawton, M., Kasten, M., May, M.T., et al.: Validation of conversion between mini-mental state examination and Montreal cognitive assessment. Mov. Disord. **31**, 593–596 (2016)